Ofioliti, 2021, 46 (2), 107-116 - doi: 10.4454/ofioliti.v46i2.541

CAN THE SCALE OF OBSERVATION HIDE COMPLEXITIES IN THE DEFORMATION HISTORY OF A TERRANE? AN EXAMPLE FROM THE BALMUCCIA PERIDOTITE MASSIF, IVREA ZONE (NW ITALY)

Marco Beltrando

Dipartimento di Scienze della Terra, Università degli Studi di Torino, Italy.

Keywords: *high temperature deformation; polyphase deformation; websterite; Ivrea-Verbano Zone.*

ABSTRACT

The degree of complexity in the deformation history of a metamorphic terrane, as unravelled by structural studies, can vary considerably according to the scale of observation. Here we report a case from the Balmuccia peridotite massif, where microstructural observations on the websteritic dykes reveal that they recorded a two-stage deformation history. Lattice Preferred Orientations (LPO) measured in the peridotitic host rock indicate that the oldest deformation was characterized by sinistral simple shear while the youngest by pure shear flow regimes. However, the distribution of folded, stretched and folded-then-stretched dykes at the outcrop scale follows a pattern concordant with large strain accommodated by pure shear only. On the other hand, the only indication of a more complex evolution is provided by the uneven dyke distribution, which is inferred to be inherited from an older deformation event. In order to define the orientation of the dykes prior to the last deformation event, a backward restoration is presented. Integrating micro- and meso-structural observations, the relative orientation of the flow plane for the first deformation event and the strain ellipse for the second has been assessed. This approach resulted in the determination of a two-stage evolution for the Balmuccia peridotite. This local evolution allows discussing wider speculations on the late Paleozoic tectonics. The Balmuccia massif, while being deformed in a flow regime characterized by sinistral simple shear, presumably during a late-Variscan lithospheric-scale extensional event, was intruded by synkinematic Al-augite websterites. As extension continued, in the Early Permian, the massif was deformed by nearly pure shear flow and large horizontal stretching could bring the Balmuccia massif to lower crustal depths.

INTRODUCTION

The quantitative reconstruction of the parameters of the deformation undergone by a rock mass through the study of deformed dyke sets is a well-established method in structural geology. Passchier (1990) has thoroughly investigated the potential of this method, showing how the distribution of sectors with shortened, stretched and shortened-then stretched dykes can be used to assess the nature of progressive deformation, provided that the rock mass has undergone a single deformation phase characterized by nearly homogeneous flow. However, complex deformation histories experienced by dyke sets may be largely overprinted by late events characterized by relatively high strain, resulting in deformation patterns that resemble those obtained through a single-stage deformation. Only microstructural observations may help unravelling these complex histories, which can be overlooked through the mesoscopic study of the dyke sets. The orientation pattern acquired by the dykes prior to the latest deformation, however, has an influence on their final distribution and may not allow discriminating between the domains with folded, stretched, folded-then-stretched dykes to be univocally defined. This, in turn, leads to difficulties in reconstructing the Mohr circles for the deformation tensor, useful to determine the flow parameters. A method based on the properties of the Mohr circle for H, the Eulerian tensor relating particle positions in the deformed state to their positions in the undeformed state (Means, 1982), allowing to overcome this problem, is here presented. In particular, this method is applied to websteritic dykes within the Balmuccia peridotite massif of the Ivrea-Verbano zone, Southern Alps. The geodynamic significance of the two latest deformation events recorded by the websteritic dykes will also be assessed.

GEOLOGICAL SETTING

The Balmuccia tectonitic peridotite crops out along the western margin of the Ivrea-Verbano zone, in the Southern Alps (Fig. 1). The Ivrea-Verbano zone is composed, west to east, by mantle peridotite slices enclosed by a mafic igneous complex and by a metasedimentary sequence, which have undergone high-grade metamorphism during the late-Variscan to Permian extensional events (Handy et al., 1999). The regional foliation and the lithologic contacts, originally flat lying, are now steeply dipping, as a result of the Alpine tilting which brought them to the present sub-vertical position (Zingg et al., 1990). The Balmuccia peridotite massif is part of an alignment of km-sized mantle bodies located in close proximity to the Insubric Line, within the bottom of the Layered Gabbro Complex (Lensch, 1971; Ernst, 1978). It hosts many mafic-ultramafic dykes, which can be grouped into a Cr-diopside websterite suite, an Al-augite websterite suite and a gabbro suite (Fig. 2 and 3) (Capedri et al., 1977; Garuti et al., 1979; Shervais, 1979a; 1979b; Comin-Chiaramonti et al., 1982; Sinigoi et al., 1983; Shervais and Mukasa, 1991; Mukasa and Shervais, 1999). Besides, for their mineralogy, the three suites differ for their relative age of intrusion. Based on crosscutting relationships, the Cr-diopside suite has been determined to be older than the Al-augite suite, which is in turn older than the gabbro suite (Mukasa and Shervais, 1999). Chemical trends indicate that the Al-Augite suite is a more evolved product of the crystallization of an ocean island basalt (OIB)-like magma, similar to the one from which the Cr-diopside suite crystallized at higher depth (see also Sinigoi et al., 1983). Since the gabbroic dykes only crop out within a short distance from the contact between the tectonitic peridotite and the surrounding rocks of the Layered Gabbro Complex and display little or

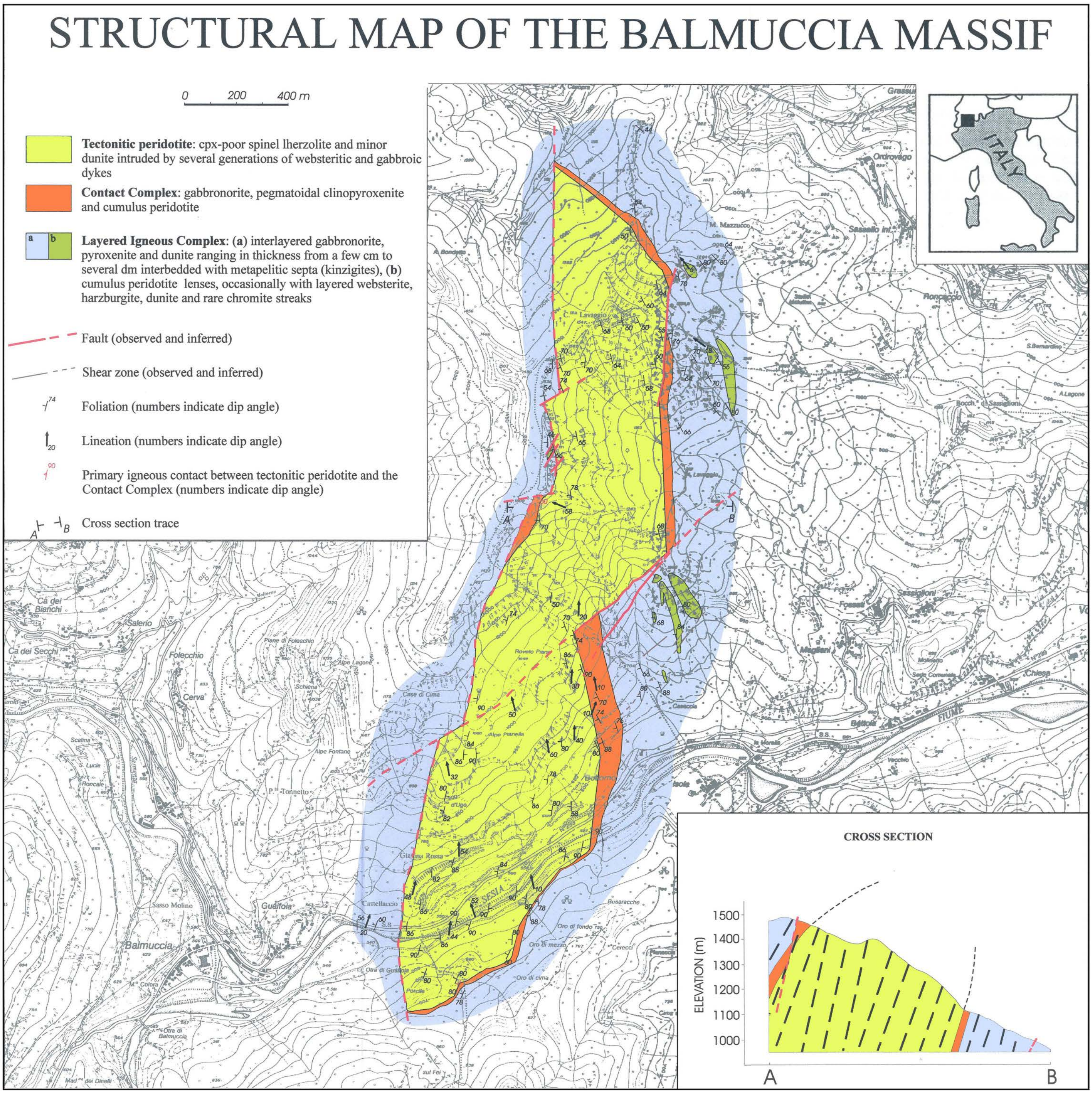

Fig. 1 - Geological map of the Balmuccia massif and surrounding rocks. Symbols indicate foliation dip, numbers indicate angle of dip. Dashed line is the trace of the cross section,

no deformation, their intrusion has been considered as having occurred late in the tectonic history of the massif. This conclusion is also supported by their MORB-like isotopic composition, different from the OIB-like isotopic signature of the websteritic dykes. Mukasa and Shervais (1999) interpreted this difference as resulting from the progressive tectonic thinning of sub-continental lithospheric mantle, inducing a switch in the origin of magma from the base of the lithosphere, for OIB-like magmas, to the underlying asthenosphere, for MORB-like magmas.

MICROSTRUCTURES

The Balmuccia tectonitic peridotite is characterized by two microstructural types: the porphyroclastic (Type-1) and the equigranular tabular (Type-2) (Mercier and Nicolas, 1974). The former is mainly preserved in the south-western sector of the massif and is characterized by the presence of three grain size families (Fig. 4A-C): 1) ribbon-shaped plurimm crystals elongated parallel to the foliation with an aspect ratio up to 6:1, strongly undulose extinction, kink walls and

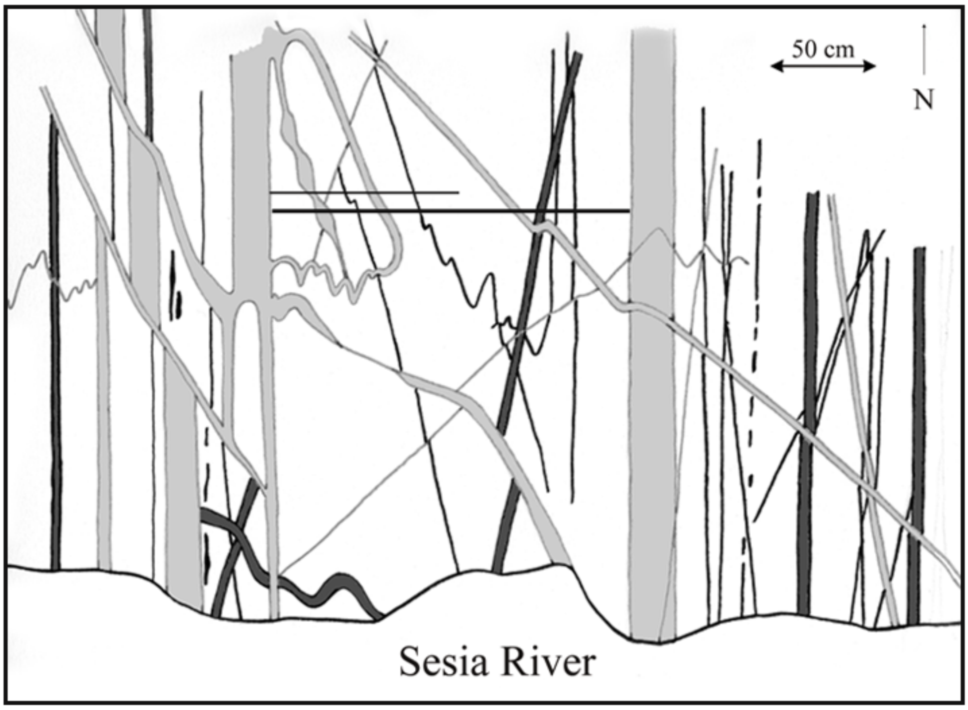

Fig. 2 - Selected outcrop with the intrusion relationships between the two websterite suites. Black- Cr-diopside websterites; grey- Al-augite websterites. Note the sinistral displacement accommodated by the Al-augite websteritic dyke (see also Fig. 3B).

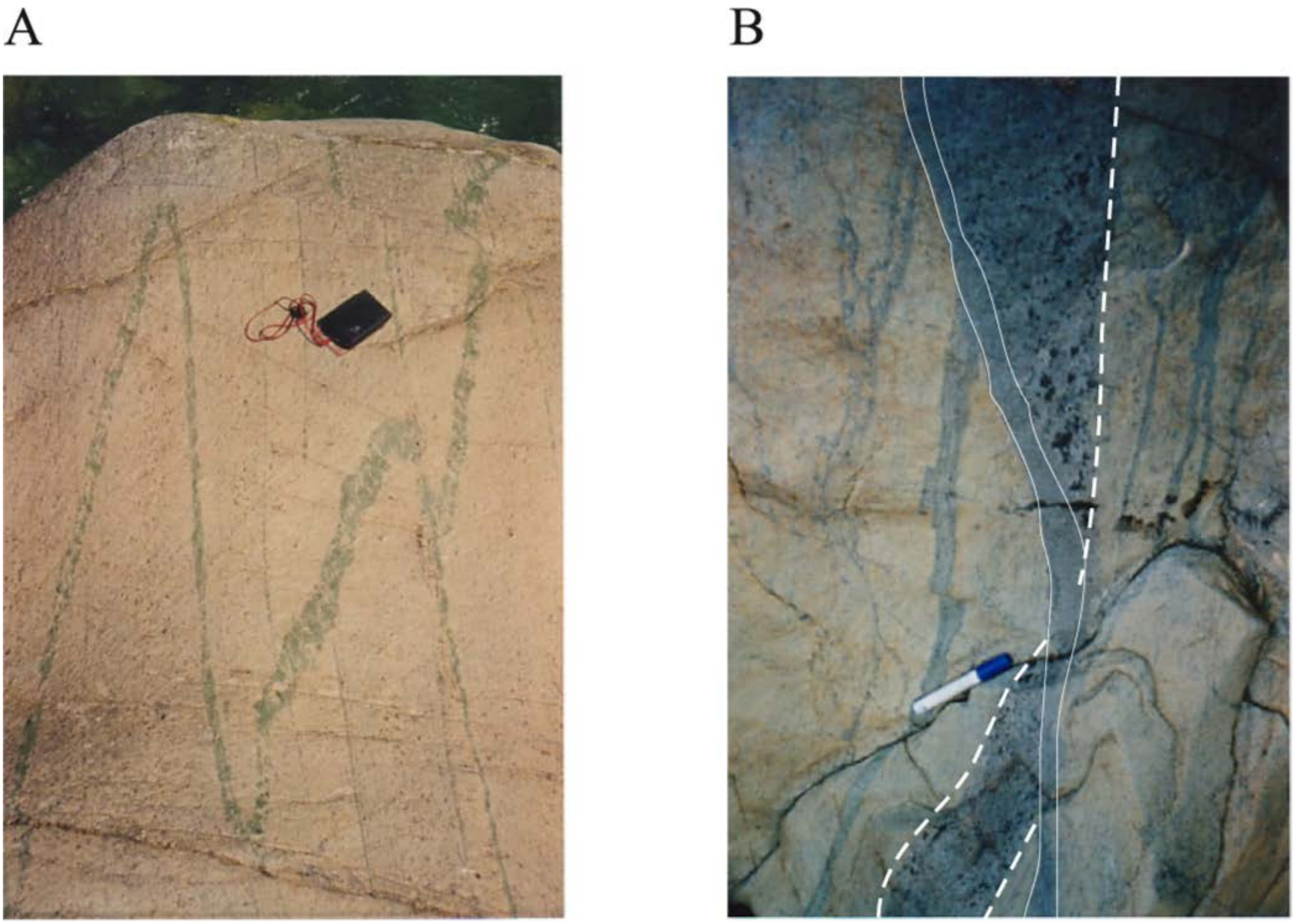

Fig. 3 - (A) Cr-diopside websteritic dyke ptygmatically folded; (B) Al-augite websteritic dyke with large spinels (black spots) displaced along the younger dyke cutting across it.

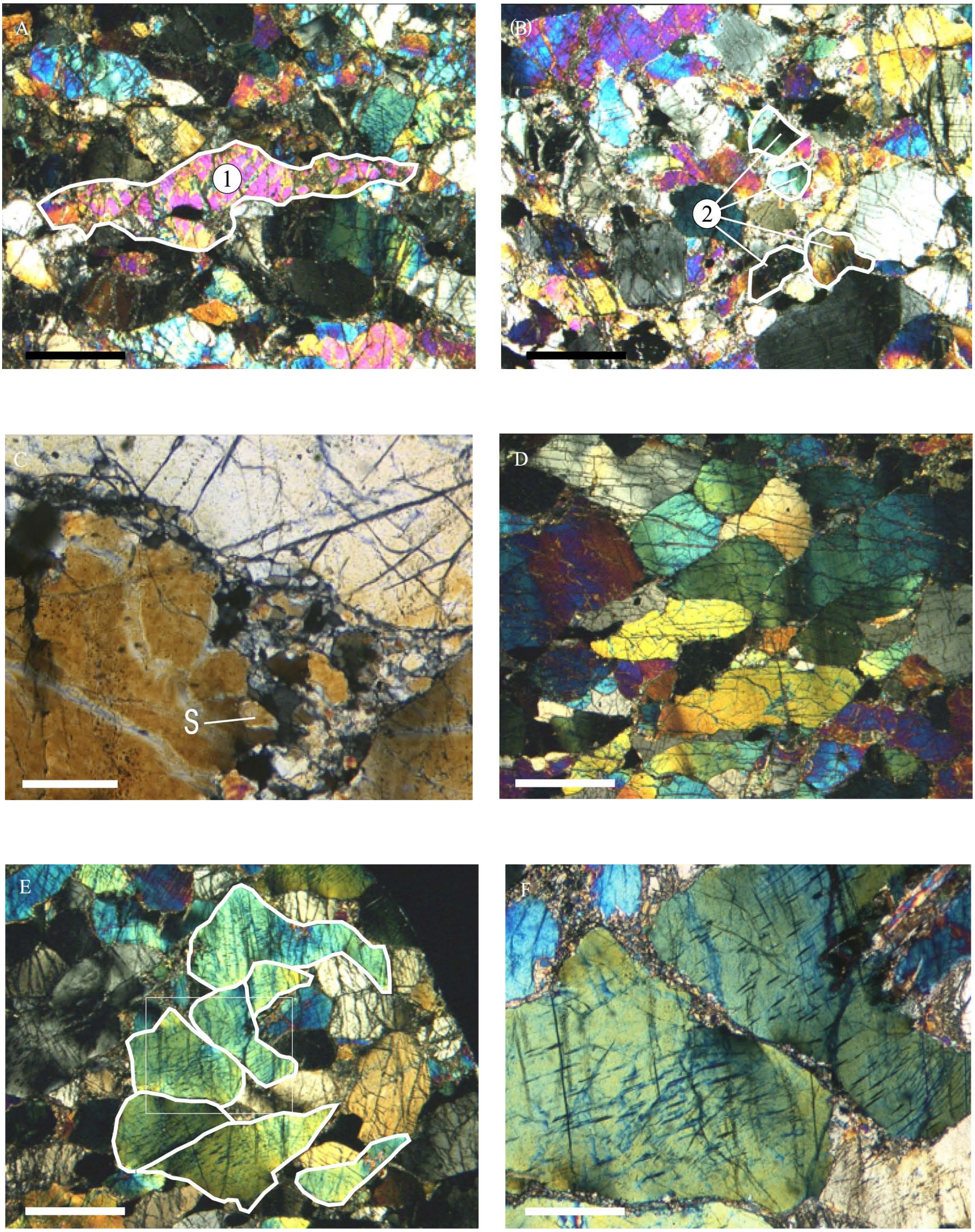

Fig. 4 - Outline of the microstructures found in the peridotite and in the websteritic dykes: (A) and (B) porphyroclastic microstructure in peridotite, with porphyroclasts strongly elongated parallel to the foliation (Type-1 crystals) and some smaller olivines (Type-2 crystals), all surrounded by abundant very fine grained crystals, originated by subgrain rotation; (C) subgrains (S) in porphyroclastic peridotite olivine. Note the same grain size as the newly recrystallized olivines along the rim; (D) tabular equigranular microstructure in peridotite; (E) former pluri-mm sized Cr-diopside recrystallized into many sub -mm sized crystals with the contacts mantled by thin layers of very fine grained Cr-diopside; (F) detail of the thin layer of very fine grained Cr-diopside crystals. Scale bar is 500 µm in (A), (B), (D) and (E), 150 µm in (F) and 60 µm in (C).

deformation lamellae; 2) lozenge shaped mm-sized crystals, less deformed, often grouped in orientation families; 3) trails of crystals less than 30μm across located at the margins of type-1 and -2 olivines, clearly originated by subgrain rotation recrystallization. Lattice Preferred Orientation (LPO) of Type-1 and Type -2 crystals indicates that they were deformed in a sinistral simple shear flow regime. The pattern distribution represented in Fig. 5 also reveals that the olivine crystals were deformed through the operation of the (010) [100] slip system, which is considered the predominant slip system at T ~ 1000°C (Skrotzki et al., 1990; Drury and Fitzgerald, 1999).

The equigranular tabular microstructures (Fig. 4D) are most common in the northeastern part of the massif and are almost ubiquitously found near the primary contact with the gabbroic rocks located to the east of the massif. Tabular olivine crystals define a steep foliation parallel to the one observed in the gabbroic rocks. LPO of newly crystallized olivine crystals (Fig. 5), with a sharp [a]-axes maximum coinciding to the spinel lineation, indicate that recrystallization occurred under pure shear flow (Boudier et al., 1984). It was proposed that the tabular equigranular microstructures formed in response to grain boundary migration recrystallization enhanced by aqueous fluids. The basic melt, whose underplating was coeval with the late-Variscan to Permian extension that affected the Ivrea-Verbano crust (Handy et al., 1999), was suggested as the probable source of the aqueous fluids (Boudier et al., 1984). On the other hand, the areas of the massif that were not reached by these fluids accommodated deformation through subgrain-rotation recrys-

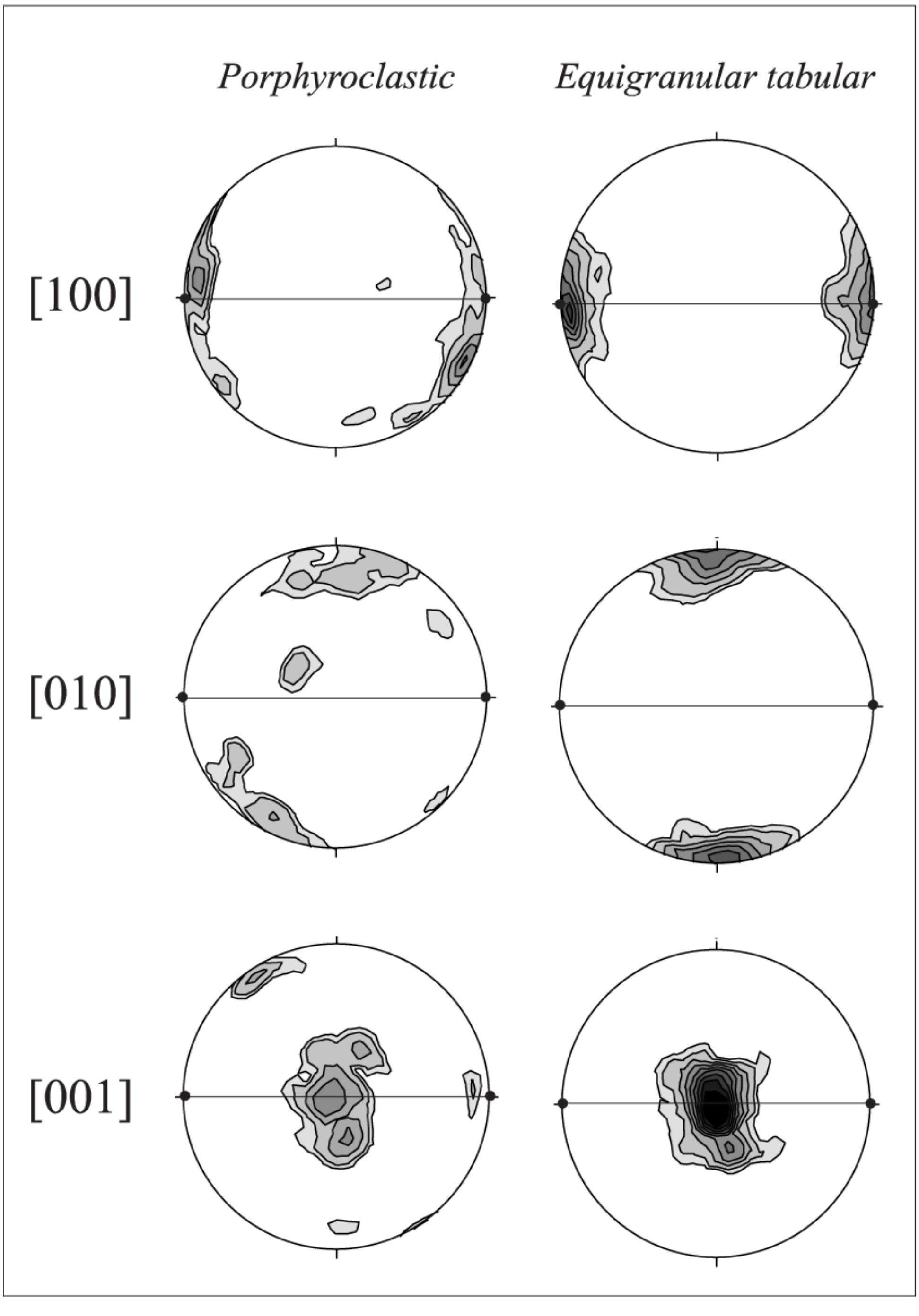

Fig. 5 - Olivine lattice preferred orientation in porphyroclastic (A) and equigranular tabular (B) lherzolites. Lower hemisphere projections (100 measurements); contours 2, 3, 5, 7 9, 11, 13, 15%.

tallization along the margins of the pre-existing olivine crystals, ultimately resulting in porphyroclastic microstructures (Boudier et al., 1984).

Samples of the websteritic dykes display the same grain size distribution observed in the porphyroclastic peridotite, with originally pluri-mm sized clinopyroxenes that recrystallized into aggregates of sub-mm crystals (Figs. 4E and F). Then, very fine-grained trails of neoblasts formed at the margins of the pyroxenes (Fig. 4F). Hence, the microstructural evolution of the dykes and the enclosing peridotites can be summarized as follows (Fig. 6). Originally, pluri-mm crystals were deformed and recrystallized into mm-sized crystals in a simple shear regime at T ~ 1000°C. A subsequent event at lower T and/or higher strain rates induced the recrystallization through subgrain rotation into fine grained (~30μm) crystals.

DYKES

The structural relationships between the different dyke suites, with Al-augite dykes consistently cutting across Cr-diopside dykes, have been portrayed in Fig. 2. It can readily be noted that every suite comprises several generations, suggesting that the intrusions occurred in many distinct pulses. Up to 20-30 cm of sinistral displacement has been accommodated by the youngest generation of Al-augite dykes (see also Fig. 3B). The orientations of the Cr-diopside and Al-augite websterites have been plotted in two stereograms, where a distinction has been made between stretched, folded and folded-then-stretched dykes (Fig. 7). The distribution of the different domains is roughly symmetric with respect to the foliation, thus suggesting that the observed deformation pattern was solely generated during the pure shear flow regime in which the regional foliation formed. This observation is clearly at odds with the deformation history obtained from the microstructural observations carried out for the tectonic peridotites.

BACKWARD RECONSTRUCTION OF THE MOHR CIRCLE FOR THE EULERIAN TENSOR H

The presence of folded-then-stretched dykes has been undoubtedly assessed only for the Cr-diopside websterites (Fig. 7), thus making them suitable for the backward structural reconstruction. Being H the Eulerian tensor relating particle positions in the deformed state to their positions in the undeformed state, a method to determine the orientation of the dykes prior to the last deformation by using the Mohr circle, is now presented. It should be noted that one boundary between the areas with folded, stretched and folded-then-stretched dykes out of four cannot be properly defined (i.e. the NE-SW oriented dykes are lacking). This results in the impossibility to discriminate between the folded and the folded-then-stretched dykes (La_1) to be drawn.

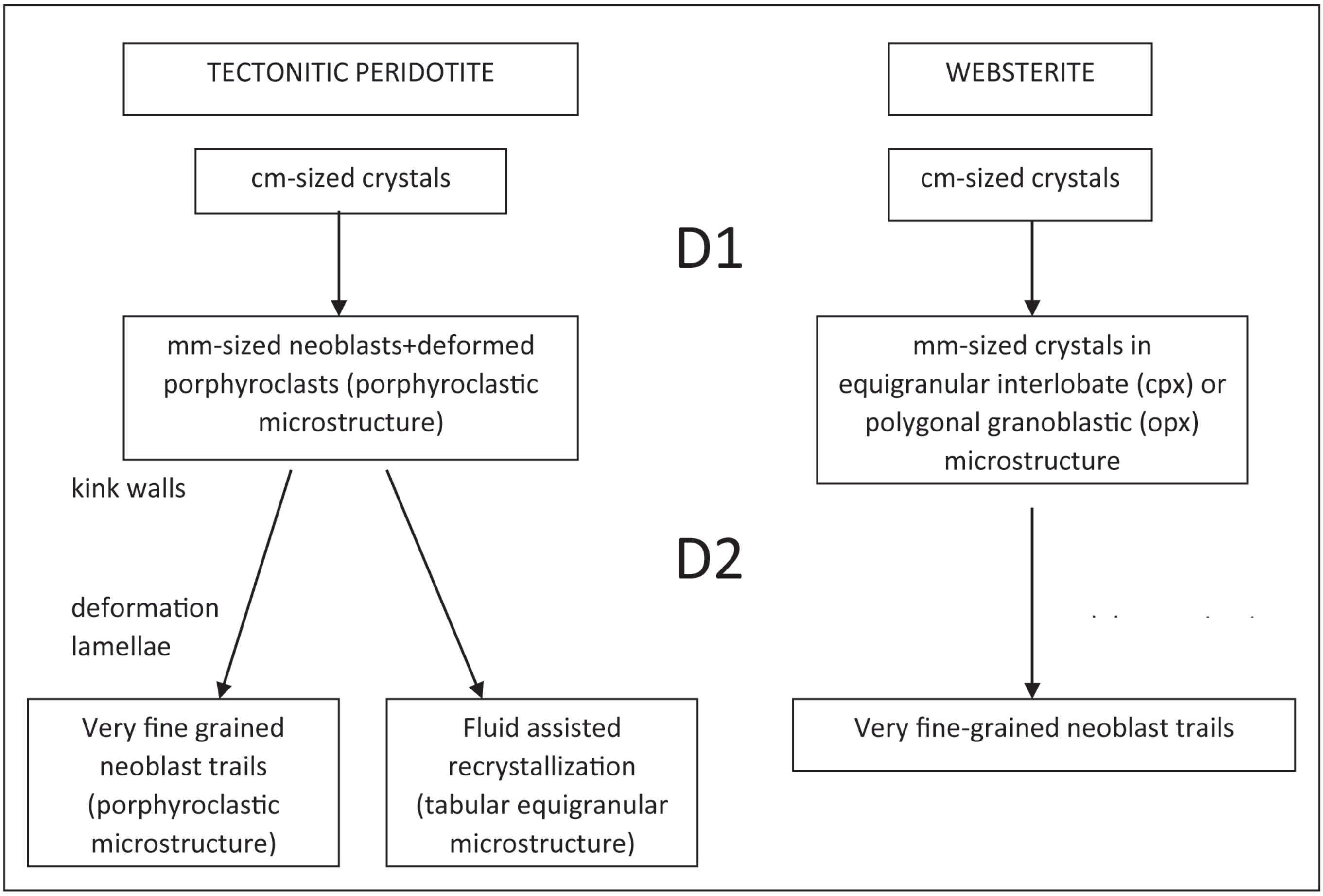

Fig. 6 - Comparison between the characteristic microstructures, which developed during D1 and D2 in the mantle peridotite and in the websteritic dykes. The effects of deformation on the porphyroclasts is shown beside arrows.

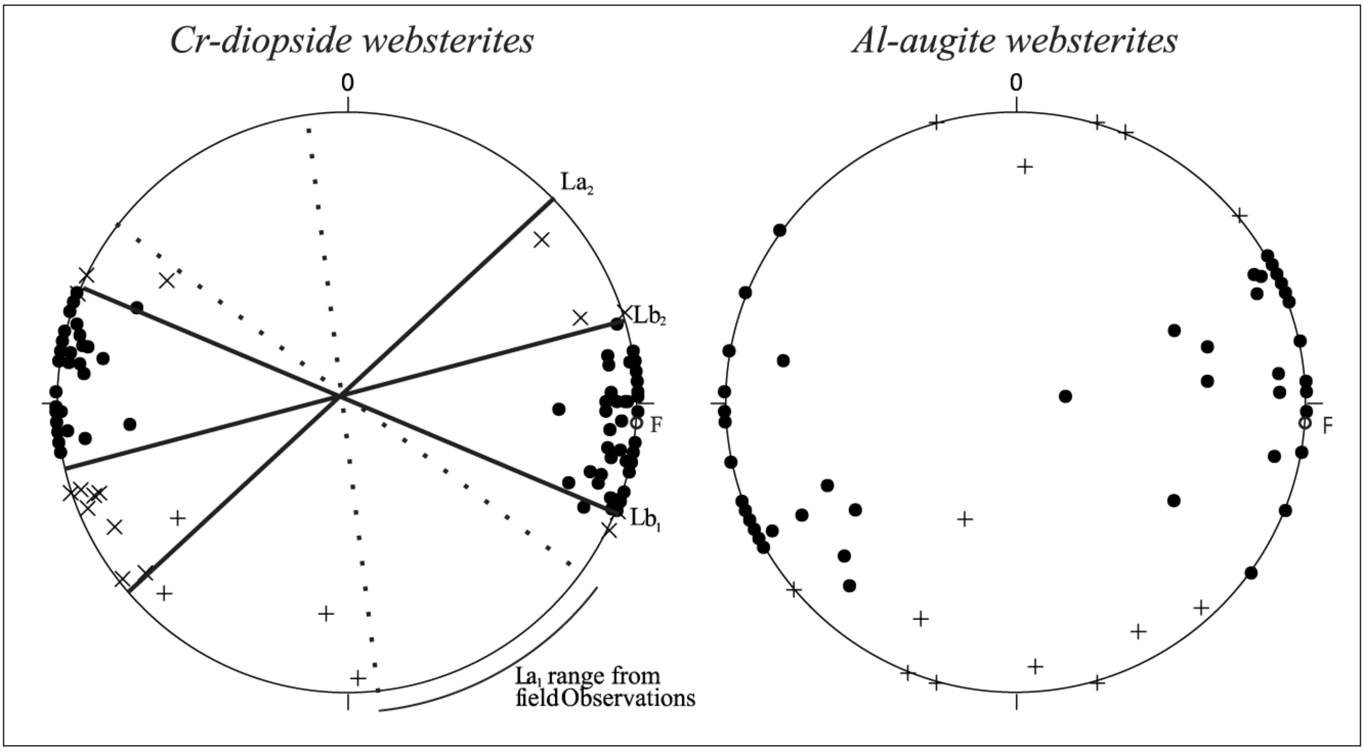

Fig. 7 - Stereograms with the orientation poles of the Cr-diopside websteritic dykes (A) and of the Al-augite websteritic dykes (B). •- stretched dykes; +- folded dykes; X- folded-then-stretched dykes, °- average foliation pole (F). Lower hemisphere projections.

However, this gap can be overcome by performing a backward reconstruction of the Mohr circle for stretch, as already outlined by Passchier (1990). In fact, the Mohr circle for H, the Eulerian tensor relating particle positions in the deformed state to their positions in the undeformed state, can still be drawn following this procedure (Fig. 8):

1- define the orientations of Lb_1, Lb_2, La_2 and the foliation plane (F) in the deformed rock. La and Lb are the lines of no instantaneous longitudinal strain at the end and at the onset of the deformation, respectively. They are material lines that separate sectors of instantaneous shortening and extension; Passchier, 1990);
2- in a Mohr diagram of arbitrary size label points Lb_1, Lb_2, La_2 and F (Fig. 8A);
3- draw tie-lines La_2-Lb_1 and F-C (being C the centre of the circle) (Fig. 8B);
4- draw the normal to the tie-line La_2-Lb_1 and lengthen F-C. Their intersection marks the origin of the Mohr space (Fig. 8B);
5- draw a tie-line from the origin of the Mohr space to Lb_2 (Fig: 8C);
6- draw a perpendicular to it passing through Lb_2. Its intersection with the Mohr circle marks La_1 (Fig. 8C);
7- draw the perpendicular to La_1-La_2 from the origin of the Mohr space. It is the horizontal reference axis (Fig. 8D);
8- raw a line parallel to La_1-La_2 from the origin of the Mohr space. It is the vertical reference axis (Fig. 8D).
9- calculate the scale of the Mohr diagram (Fig. 8E and F) using the equation (Passchier, 1990): $\cos(La_1 \wedge La_2) = N[\ln(M+N) + \ln(M-N)]/R[\ln(M+N) - \ln(M-N)]$, where $La_1 \wedge La_2$ is the angle between La_1 and La_2 measured in real space.

The strain ratio for the latest deformation can now be characterized quantitatively (Passchier, 1990), resulting in $R_f = 3.4$. The newly found orientation of La_1 (Fig. 8C) can be drawn in the stereogram with the Cr-diopside dyke distribution (Fig. 9), resulting in a roughly symmetric distribution of the different domains with respect to the foliation. This distribution points towards a nearly pure shear flow as responsible for the deformation pattern. Furthermore, the four components of the position gradient tensor **H** can be determined from its Mohr circle. Choosing a line parallel to the NS direction in the geographic space as our reference line, using the conventions of Means (1982):

$$H = \begin{vmatrix} 0.58 & 0.28 \\ 0.00 & 2.03 \end{vmatrix}$$

Applying this deformation tensor to the orientation pattern obtained from field studies of the Cr-diopside and Al-augite websterites, their orientation prior to the latest deformation can be determined (Fig. 10).

DISCUSSION

Nicolas and Jackson (1983) showed that the occurrence of a single set of shear planes, along which dykes intrude, is indicative of simple shear deformation. In a rock mass undergoing deformation by any other flow type, two sets

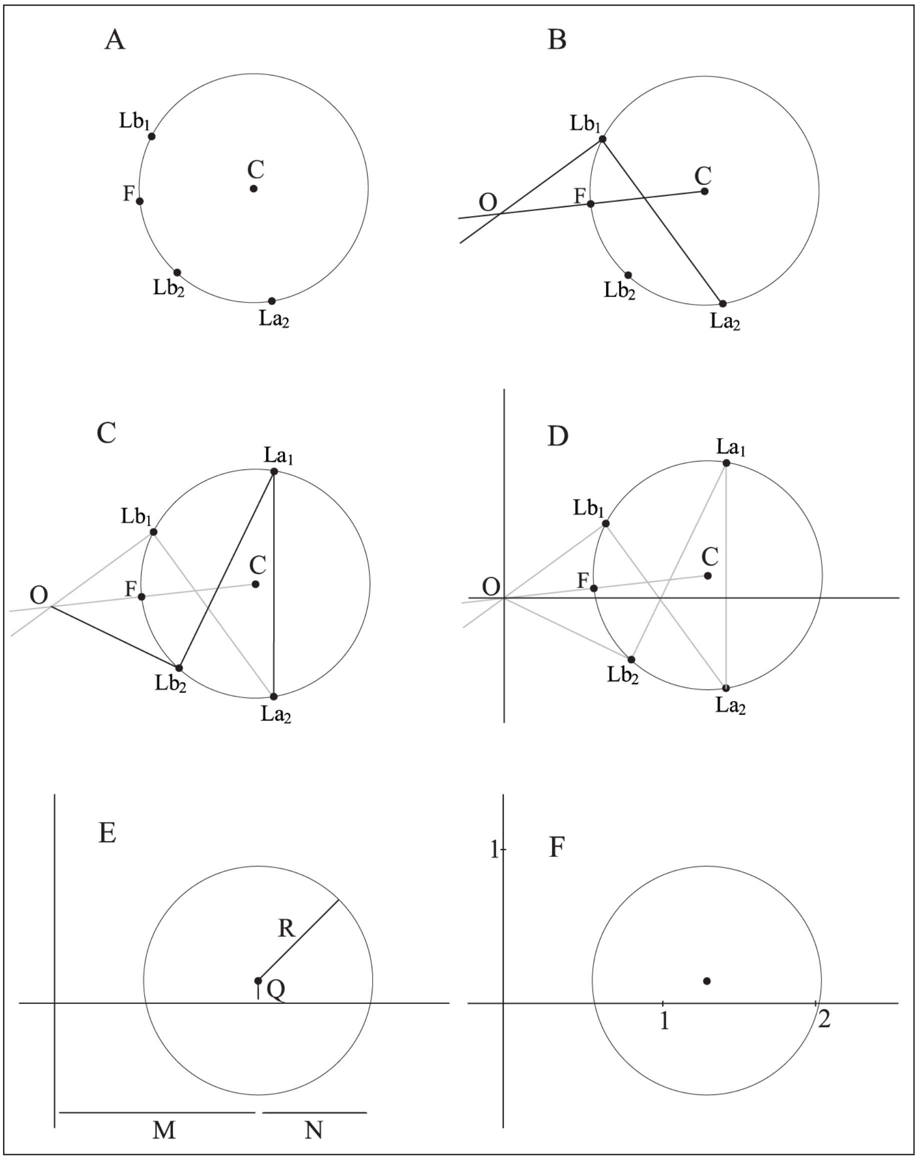

Fig. 8 - Reconstruction of the Mohr circle for H from a set of deformed dykes. Three boundaries of sectors of folded, stretched and folded-then-stretched dykes out of four are plotted, together with the foliation (A). Tie lines are then drawn to find the origin of the reference frame (B) and the position of the fourth unknown boundary (C). The reference frame is drawn (D) and the scale on the reference axes is thus established (E, F). M, N, Q and R are the line segments allowing to calculate the scale of the diagram, as defined by Passchier (1990).

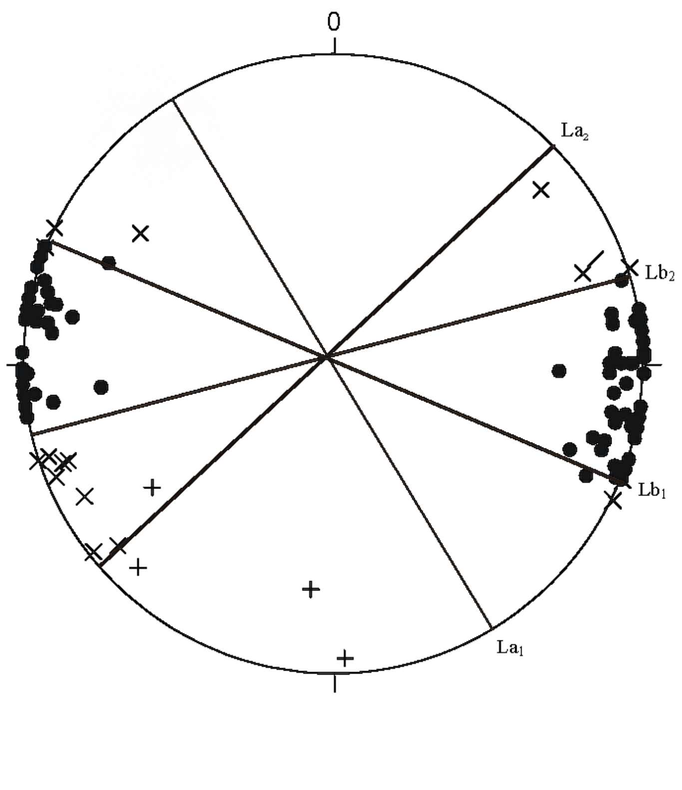

Fig. 9 - Stereogram with the orientation poles of the Cr-diopside websteritic dykes. Also drawn are the boundaries between the domains with stretched and folded-then-stretched dykes (Lb_1 and Lb_2) and the domains with folded and folded-then-stretched dykes (La_1 and La_2).

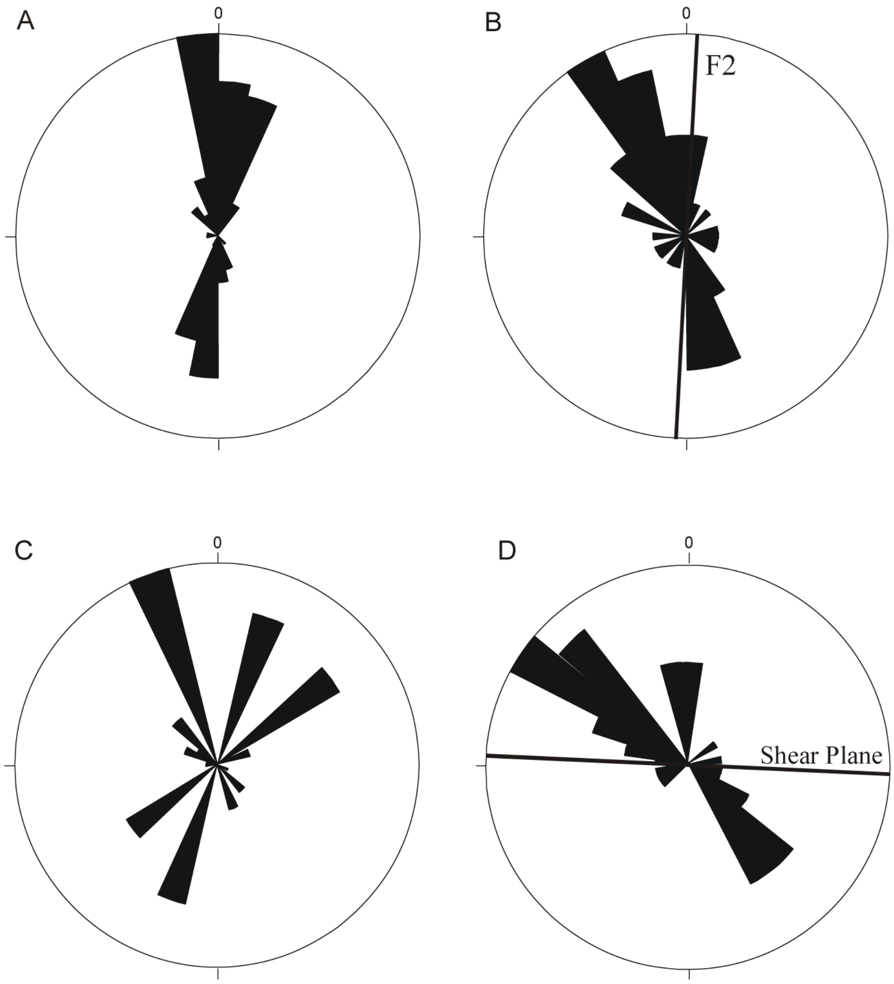

Fig. 10 - Rose diagrams with the distribution of the Cr-diopside websteritic dykes (A, C) and the Al-augite websteritic dykes (B, D) after (A, B) and before (C, D) the latest deformation event. In D the supposed orientation of the shear plane of D1 has been drawn. F2- foliation observed in the field.

of shear planes should instead form. The occurrence of Al-augite dykes accommodating up to 20-30 cm of sinistral displacement (Figs. 2 and 6B) in several locations indicates that at least the youngest generation of Al-augite dykes intruded a rock mass that was undergoing deformation by sinistral simple shear. However, the latest deformation event, responsible for the observed dyke distribution, was characterized by nearly pure shear flow, as indicated by the nearly symmetric deformed dyke pattern with respect to the foliation and by the LPO in the equigranular domain (Fig. 5). Therefore, the Al-Augite dykes must have intruded during an older deformation phase characterized by different flow parameters, namely during sinistral simple shear. This interpretation is consistent with the flow regime obtained from LPO in olivine from the host rock (Fig. 5). In such rotational regime, all material lines would progressively rotate towards the shear plane, which acts as a fabric attractor. The amount of rotation experienced by the Cr-diopside websteritic dykes is likely to be higher that for the Al-Augite websteritic dykes, whose intrusion was synkinematic. Hence, the position of the shear plane for D1 can be qualitatively estimated at a small anticlockwise angle from the Cr-diopside dyke orientation maximum (Fig. 10) and at a small clockwise angle from the Al-Augite dyke orientation maximum. This results in the flow plane for D1 lying at a small angle to the foliation that formed during D2.

CONCLUSIONS

This study shows that deformation patterns seemingly formed in response to a single deformation event may in fact result from the superposition of a relatively high-strain deformation over a pre-existing pattern. The inherited orientation pattern may eventually hinder to draw the divide between domains with folded, stretched or folded-then-stretched dykes. A method that allows overcoming the aforementioned problem, provided that only one line of no instantaneous longitudinal strain out of four cannot be properly defined, has been developed. When the flow responsible for the observed deformation pattern is quantitatively characterized, its effects can be subtracted in order to obtain the dyke orientation prior to it. Integrating this dyke distribution with other field and microstructural observations, the relative orientation of the finite strain ellipsoids for the two latest deformation events experienced by the dykes can be determined.

This method, applied to the websteritic dykes of the Balmuccia tectonitic peridotite, resulted in the determination of a multi-stage evolution for the massif: a mantle peridotite, which already hosted Cr-diopside websterites, underwent a first deformation event characterized by sinistral simple shear, with syn-kinematic intrusion of the Al-augite websterites, and a second event characterized by nearly pure shear flow. The interpretation of this two-stage history can be twofold (Fig. 11):

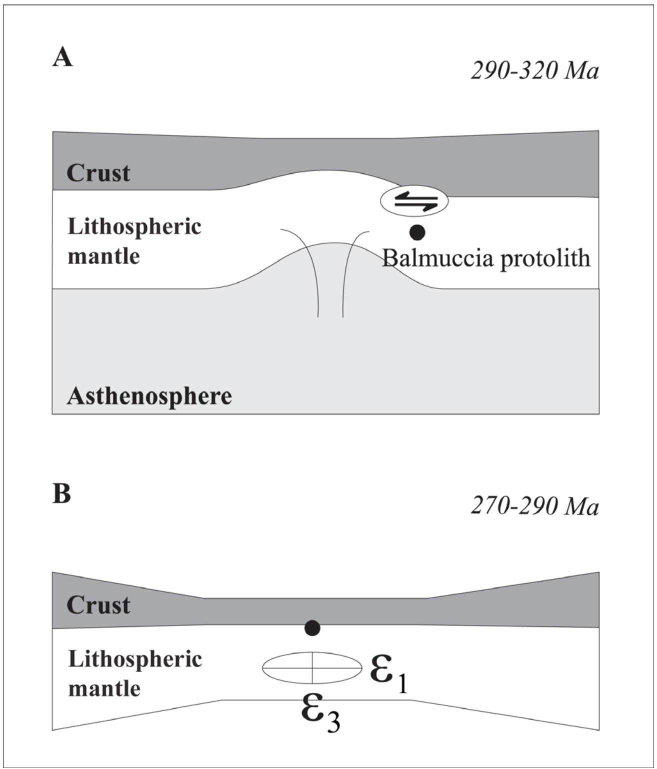

Fig. 11 - Schematic evolution of the Balmuccia massif, here represented by the black dot, from its ascent in the mantle (A) leading to the lithospheric emplacement, to the lithospheric thinning (B), which brought it in contact with crustal rocks. The age of the lithospheric thinning is from Handy et al. (1999), according to interpretation (1) reported in the Conclusions. Ellipses represent finite strain.

1- The first deformation event could be related to the late-Variscan lithospheric extension that affected the Ivrea-Verbano Zone at ca. 290-320 Ma, followed by a Permian transtensional episode at ca. 270-290 (Handy et al., 1999). The two aforementioned stages were characterized by different flow regimes. This progressive deformation is also consistent with the tectonic thinning of subcontinental lithospheric mantle during continuous extension proposed by Mukasa and Shervais (1999) to account for the change in the source region of mantle-derived magmas from ocean island basalt (OIB)-like lithosphere to the underlying MORB asthenosphere.

2- Alternatively, the two deformation events were unrelated. The older one could reflect horizontal simple shear flow under mantle conditions, possibly as part of a horizontal branch of a convective cell, whereas the younger deformation event could be related to a poorly defined event of late-Variscan to Permian lithospheric extension.

ACKNOWLEDGEMENTS

Several versions of this article of Marco Beltrando were found by RC in his personal computer. The most recent version of the draft was sent for an opinion to Prof. Ceers Paschier, Editor-in-chief Emeritus of the Journal of Structural Geology, who found it interesting and worthy of publication. The Editors of this Ofioliti special section express their gratitude to Matteo Maino and Silvano Sinigoi for reviewing the early version of this manuscript. The Editors carried out minor changes to text, in agreement with the reviewers' suggestions.

REFERENCES

Boudier F., Jackson M. and Nicolas A., 1984. Structural study of the Balmuccia massif (Western Alps): a transition from mantle to lower crust. Geol. Mijnb., 63: 179-188.

Capedri S., Garuti G., Rivalenti G. and Rossi A., 1977. The origin of the Ivrea-Verbano basic formation- pyroxenitic and gabbroic mobilisates as product of partial melting of mantle peridotite. N. Jb. Miner. Mh., 4: 168-179.

Comin-Chiaromonti P., Demarchi G. and Sinigoi S., 1982. Relazioni tra fusione e deformazione nella peridotite di Balmuccia. Rend. Soc. It. Miner. Petrol., 38: 685-700.

Drury M.R. and Fitzgerald J.D., 1998. Mantle rheology: insights from laboratory studies of deformation and phase transition. In: I. Jackson (Ed.), The Earth's mantle: composition, structure and evolution. Cambridge Univ. Press, p. 503-549.

Ernst W.G., 1978. Petrological study of lherzolitic rocks from the Western Alps. J. Petrol., 19: 391-342.

Garuti G, Rivalenti G., Rossi A. and Sinigoi S., 1979. Mineral equilibria as geotectonic indicators in the ultramafics and related rocks of the Ivrea-Verbano basic complex (Italian Western Alps): pyroxenes and olivine. Mem. Sci. Geol. Padova, 33: 147-160.

Handy M.R. Franz L., Heller F., Janott B. and Zurbriggen R., 1999. Multistage accretion and exhumation of continental crust (Ivrea crustal section, Italy and Switzerland). Tectonics, 18: 1154-1177.

Lensch G., 1971. Die Ultramafitite der Zone von Ivrea. Ann. Univ. Saraviensis, 9: 5-146.

Means W.D., 1982. An unfamiliar Mohr circle construction for finite strain. Tectonophysics, 89: T1-T6.

Mercier J.-C. and Nicolas A. 1974. Textures and fabrics of upper-mantle peridotites as illustrated by xenoliths from basalts, J. Petrol., 16: 454-487.

Mukasa S.B. and Shervais J.W., 1999. Growth of subcontinental lithosphere: evidence from repeated dyke injections in the Balmuccia lherzolite massif, Italian Alps, Lithos, 48: 287-316.

Nicolas A. and Jackson M.D., 1983. Dike structure in mantle peridotites: injection mechanisms and relation to plastic flow. J. Petrol., 23: 568-582.

Passchier C.W., 1990. Reconstruction of deformation and flow parameters from deformed vein sets. Tectonophysics, 180: 185-199.

Shervais J.W., 1979a. Ultramafic layers in the alpine-type lherzolite massif at Balmuccia, NW Italy. Mem. Sci. Geol. Univ. Padova, 33: 135-145.

Shervais J.W., 1979b. Thermal emplacement model for the Alpine lherzolite massif at Balmuccia, Italy. J. Petrol., 20: 795-820.

Shervais J.W. and Mukasa S.B., 1991. The Balmuccia orogenic lherzolite massif, Italy. J. Petrol., Special Lherzolite Iss., p. 155-174.

Sinigoi S., Comin-Chiaramonti P., Demarchi G. and Siena F., 1983. Differentiation of partial melts in the mantle: evidence from the Balmuccia peridotite, Italy. Contrib. Miner. Petrol., 82: 351-359.

Skrotzki W., Wedel A., Weber K. and Müller W.F., 1990. Microstructure and texture in lherzolites of the Balmuccia massif and their significance regarding the thermomechanical history. Tectonophysics, 179: 227-251.

Zingg A., Handy M.R., Hunziker J.C. and Schmid S.M., 1990. Tectonometamorphic history of the Ivrea zone and its relationship to the crustal evolution of the Southern Alps. Tectonophysics, 182: 169-182.

Received, February 1, 2021
Accepted, May 12, 2021